Applications of Wavelet Analysis for Determining Glucose Concentration of Aqueous Solutions Using NIR Spectroscopy

Christopher S. McNulty, Ganapati Mauze
Analytical/Medical Laboratory
HPL-98-53
March, 1998

E-mail: ganapati_mauze@hpl.hp.com
cmcnulty@mit.edu

wavelets, glucose, NIR spectroscopy, noninvasive, diabetes

A method for predicting clinically relevant levels of glucose concentration in aqueous solutions from NIR absorbance spectra will be described. The method makes use of the discrete wavelet transform (DWT). The general concepts of the DWT will be briefly reviewed, with emphasis on the properties of the DWT that make it a suitable transform for the analysis of spectroscopic data. The wavelet analysis prediction method will then be described. Results obtained from applying this method to a set of spectra obtained from solutions with varying glucose and protein concentrations will be presented. These results will be compared with the results obtained from using partial least-squares regression (PLSR).

Internal Accession Date Only

To be presented at *BiOS '98 (Biomedical Optics),* San Jose, California, January 29, 1998.

Applications of wavelet analysis for determining glucose concentration of aqueous solutions using NIR spectroscopy

Christopher S. McNulty and Ganapati Mauze

Hewlett-Packard Laboratories, 3500 Deer Creek Road, Palo Alto, CA 94304

ABSTRACT

A method for predicting clinically relevant levels of glucose concentration in aqueous solutions from NIR absorbance spectra will be described. The method makes use of the discrete wavelet transform (DWT). The general concepts of the DWT will be briefly reviewed, with emphasis on the properties of the DWT that make it a suitable transform for the analysis of spectroscopic data. The wavelet analysis prediction method will then be described. Results obtained from applying this method to a set of spectra obtained from solutions with varying glucose and protein concentrations will be presented. These results will be compared with the results obtained from using partial least-squares regression (PLSR).

Keywords: wavelets, glucose, NIR spectroscopy, noninvasive, diabetes

1. INTRODUCTION

Over the course of the last decade, a large amount of research has been performed in the area of making measurements of physiological levels of glucose concentration using NIR absorbance spectroscopy. Several characteristics of the NIR, such as known regions of glucose absorption and bands of low water absorption, make it a valuable source of glucose information. Spectra obtained from the NIR, however, are plagued in several respects. First, several other classes of chemicals present in biological fluids, such as proteins and triglycerides, also absorb highly in the regions of high glucose absorption [1,2]. Since the concentration of proteins in biological fluids is much greater than that of glucose, the signals from protein absorption can often mask the characteristic glucose absorption signals. Further, significant sources of variation in NIR absorbance spectra are also created by changes in temperature and random fluctuations of spectral baselines.

Because of the vast amount of overlapping information present in NIR spectra, researchers have employed several different multivariate filtering and regression techniques in order to predict glucose concentration. Some of the more popular techniques that have been used include Fourier filtering[3], partial least squares regression[4], and radial basis function analysis[5]. In this paper, we will present an alternative to these more traditional processing techniques involving the use of the DWT.

2. THE DISCRETE WAVELET TRANSFORM

There are two fairly different manners in which the DWT can be presented and viewed. On one hand, the DWT can be viewed as a process of successive filtering and downsampling. On the other hand, the DWT can also be viewed as a projection onto an orthogonal basis. Both views are useful for comprehension of the DWT, so we will briefly present each of them and attempt to show how they represent the same transform. More thorough descriptions of the DWT are widely available[6,7].

Starting with the filtering/downsampling view of the DWT is probably the easiest way to introduce the transform, since this process can be depicted well pictorially. In this view of the DWT, a number of successive filtrations and downsamplings are performed on a given N-point data vector, where N is equal to a power of 2. In the first step of this process, the original N-

Further Author Information -
C.S.M: Email: cmcnulty@mit.edu; Telephone: (650) 236-2248; Fax: (650) 857-2862
G.M.(correspondence): Email: ganapati_mauze@hpl.hp.com; Telephone: (650) 857-7058; Fax: (650) 857-2862

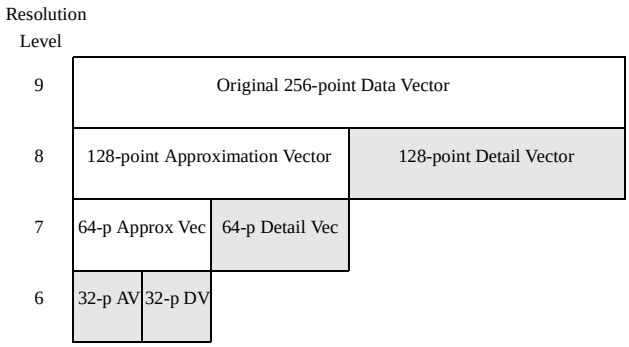

Figure 1. General scheme for the DWT decomposition of a 256-point data vector. Shaded regions make up the DWT of the original data when resolution level six is the lowest level of decomposition.

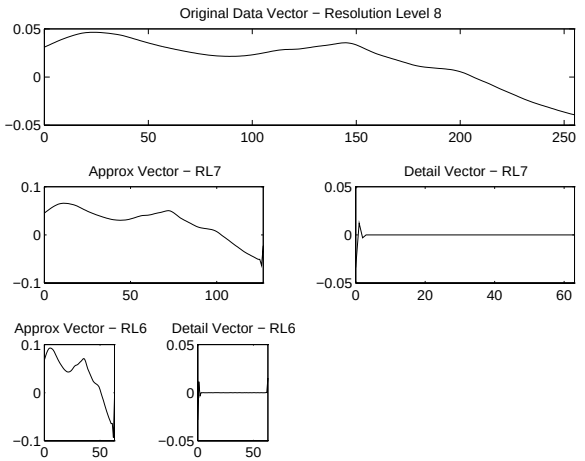

Figure 2. Three resolution levels in the DWT decomposition of an NIR absorbance spectrum.

point data vector is passed through both a low-pass filter and a high-pass filter, and then the outputs of these filters are down-sampled. The downsampled output of the high-pass filter contains details present in the data vector. This vector has N/2 points and is called the detail vector. The downsampled output of the low-pass filter, on the other hand, contains an approximation of the data vector. This vector also has N/2 points and is called the approximation vector. Together, the approximation vector and the detail vector form an N-point DWT of the original data vector.

The DWT is often carried further by performing additional filtration on the approximation vector. This additional filtration is of the same form as that which was performed on the original data vector. Even the same filters are used. Thus, the process once again yields an approximation vector and a detail vector. This time, however, these vectors only have N/4 points. The approximation vector can then be filtered and downsampled again. This process of successively filtering and downsampling approximation vectors can be carried out as many times as desirable, or until the approximation vector contains only one point. Every time that an approximation vector is decomposed into a new approximation vector and a detail vector, a new DWT is created. This new DWT consists of the newly calculated approximation vector and detail vector, along with all of the previously calculated detail vectors.

Figure 1 shows the manner in which a DWT would decompose a 256-point data vector. Every level of decomposition in the DWT is called a resolution level. By convention, each resolution level is numbered by finding the $\log_2$ of the number of points in the approximation (or detail) vector. In Figure 1, three decompositions take place, so that the lowest resolution level of the DWT is resolution level 6. The shaded boxes represent the DWT given when the decomposition process is stopped at this level.

Figure 2 shows a specific example in which a DWT was used in order to decompose an NIR absorbance spectrum. If the DWT decomposition were to stop at resolution level 6, the DWT would be made of the approximation and detail vectors of resolution level 6 and the detail vector of resolution level 7.

The above successive filtration process is one manner in which a DWT may be calculated. Because of the specific properties of the filters used in this process, however, a DWT can also be calculated as a projection onto an orthogonal basis. For the 256-point signal of Figure 1, 256 basis functions would be needed for the calculation of the DWT represented by the shaded regions. The 128 basis functions that would be used to calculate the resolution level 7 detail vector must represent the high-pass filtering and down-sampling of the original signal described above. The basis functions of other resolution levels, of course, will have to represent an even more complex process. For example, the 64 basis functions that would be used to calculate the resolution level 6 detail vector must represent the process of low-pass filtering, then down-sampling, then high-pass filtering, and finally down-sampling again.

The basis functions used in the DWT are known as wavelets. The shapes of wavelets are derived from the two filters used in the successive filering/downsampling process described above. These filters must meet specific constraints that are described in detail in the wavelet literature[7]. There are an infinite number of filters that meet these constraints, so there are an

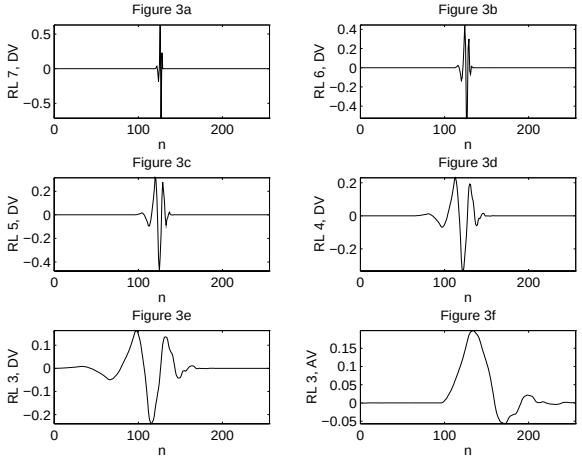

Figure 3. Eight wavelets in the D8 basis when resolution level 3 is the lowest resolution level in the DWT. The vertical axis of each plot displays the resolution level (RL) of the wavelet and whether it would be used to calculate part of a detail vector (DV) or an approximation vector (AV).

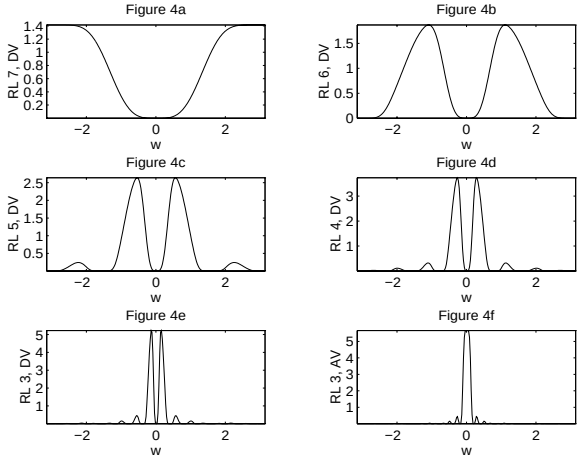

Figure 4. The magnitudes of the Fourier transforms of the wavelets shown in Figure 3. The vertical axis of each plot displays the resolution level (RL) of the wavelet and whether it would be used to calculate part of a detail vector (DV) or an approximation vector (AV).

infinite number of possible wavelet bases. Knowledge of the specific constraints on the filters and bases, however, is not as important as knowledge of the general features of wavelets. These general features include the facts that wavelets are real, aperiodic, and have nonzero values only over finite portions of their length. All of these features of wavelets are best introduced graphically.

Figure 3 shows eight wavelet basis functions in the popular wavelet basis known as Daubechies-8 (D8), with resolution level 3 as the lowest resolution level. Each of the wavelets in Figure 3 would be used in the calculation of a different resolution level detail or approximation vector. The wavelet in Figure 3a, for example, would be used to calculate one point in the resolution level 7 detail vector. The other 127 basis functions used to compute the resolution level 7 detail vector would all be simple translations of the wavelet in Figure 3a. Indeed, the basis functions of any resolution level detail or approximation vector are simple translations of each other. Thus, although Figure 3 does not display all of the wavelet basis functions in the D8 basis, it does display all of the shapes of the basis functions.

Inspection of Figure 3 should yield some information about the differences between basis functions of different resolution levels. For example, the basis functions of high resolution levels are represented very locally in space, whereas the basis functions of low resolution levels are represented over wide ranges. In other words, high resolution level basis functions have a great deal of resolution in the spatial domain, and low resolution level basis functions have low resolution in the spatial domain.

The spatial domain representation of the different wavelets in a basis yields a certain amount of information about wavelets and resolution levels. To more completely understand wavelets and resolution levels, however, it is necessary to inspect wavelets in the frequency domain. The magnitudes of the Fourier transforms of the wavelets in Figure 3 are shown in Figure 4. Just as in Figure 3, every plot in Figure 4 represents a basis function for a certain resolution level detail or approximation vector. Translations have no effects on the magnitude of Fourier transforms. Thus, the magnitude Fourier transforms of basis functions of the same resolution level detail or approximation vector are exactly the same.

The plots in Figure 4 clearly illustrate that basis functions from different resolution levels cover different frequency bands. The basis functions from higher resolution levels represent higher frequencies, whereas the functions from lower resolution levels represent lower frequencies. Figure 4 also clearly displays that the basis functions of different resolution levels display different amounts of resolution in the frequency domain. Basis functions from high resolution levels have very little frequency resolution, whereas basis functions from low resolution levels have much more frequency resolution.

When inspecting Figures 3 and 4 together, it should be evident that different resolution levels represent different amounts of trade-off between frequency and spatial resolution. The basis functions of high reoslution levels have high spatial resolution and low frequency resolution, whereas the basis functions of low resolution levels have low spatial resolution and high frequency resolution. The fact that wavelet bases contain basis functions with varying amounts of spatial and frequency resolu-

tion make them useful alternatives to untransformed or Fourier bases. Untransformed bases, on one hand, provide perfect spatial resolution but no frequency resolution. Fourier bases, on the other hand, provide perfect frequency resolution but no spatial resolution.

Now that we have discussed the general properties of wavelet basis functions, we introduce the mathematical form of the DWT. As stated above, the DWT can be calculated as a linear projection onto an orthogonal basis. This projection can be written as follows,

$$w[k] = \sum_{n=0}^{N-1} x[n]\varphi_k[n],\ k = 0, 1, \ldots, N-1$$

where x[n] is the original signal. w[n] is the DWT of x[n], and the functions $\varphi_k[n]$ are the basis functions of the N-point DWT. For our purposes, the matrix form of this equation will be more useful:

$$\mathbf{w} = \begin{bmatrix} w[0] \\ w[1] \\ | \\ w[N-1] \end{bmatrix} = \begin{bmatrix} - & \varphi_0[n] & - \\ - & \varphi_1[n] & - \\ & | & \\ - & \varphi_{N-1}[n] & - \end{bmatrix} \begin{bmatrix} x[0] \\ x[1] \\ | \\ x[N-1] \end{bmatrix} = \mathbf{Tx}$$

2. USING THE DWT IN SPECTRAL ANALYSIS

In spectral analysis, unprocessed spectra will often have their useful information spread out over many points, and this useful information usually occurs at points that are affected by interferents and noise. Thus, linear transforms are often applied to spectra in order to concentrate salient information into as few transform variables as possible while separating this information from that caused by interferents. Transforms do not add any information to the original signal. They simply manipulate the information so that it is represented in a different manner. A transform will do a good job of representing important spectral features when some of its basis functions closely resemble the spectral features of interest. In other words, a good transform will have basis functions that are well matched to the shapes of important spectral characteristics.

One of the strong points of the DWT is that infinitely many bases can be used with the transform. This freedom allows one to choose a basis that will be well suited for a specific problem. Probably the easiest way to choose an appropriate basis is to simply inspect the basis functions of several different bases and look for basis functions that match up well with the spectral features of interest.

In Figure 5, the NIR absorbance spectrum of a 400mg/dL glucose solution is plotted against a scaled basis functions of the D8 (Daubechies-8) wavelet basis. This specific basis function is used to calculate part of the resolution level 3 detail vector. It should be evident from Figure 5 that the DWT basis function is fairly well matched with the glucose signal. Other functions in this basis also match up well with the spectrum of glucose, so the D8 basis is suitable for decomposing spectra which contain glucose information. Obviously, no wavelet in this basis perfectly represents the glucose signal shown in Figure 5. The spatial locality and peaky nature of the DWT basis functions, however, do seem to make the DWT an attractive transform for the analysis of glucose absorbance spectra.

In order to compare wavelet basis functions to the basis functions of the DFT, the real part of a scaled DFT basis functions and the glucose absorbance spectrum are shown in Figure 6. Of course, the DFT offers no freedom to choose an appropriate basis for a certain application. With the DFT, one is stuck with basis functions that are nonzero over their entire length. The DFT basis function in Figure 6 appears to do a good job of representing the large glucose peak at 4400cm^{-1}. The extraneous oscillations of the basis function, however, reduce its ability to properly represent glucose information in the presence of interferents. However, just because no one DFT basis function can accurately represent glucose information does not mean that it is not a useful transform. Several different basis functions may be necessary in order to accurately represent a certain spectral feature. It does make sense, though, to use transforms with spatially localized basis functions on spectra with spatially localized spectral features.

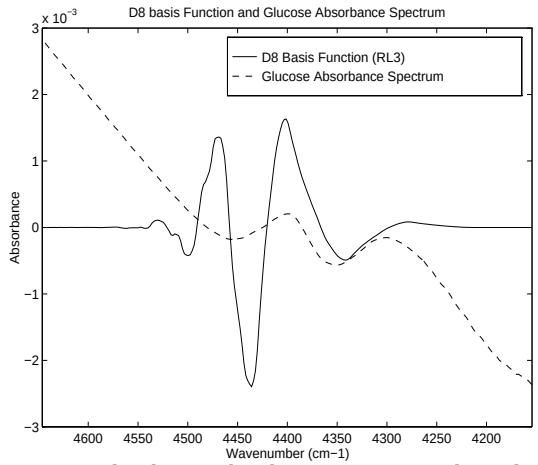

Figure 5. 400mg/dL glucose absorbance spectrum and a scaled basis function from the D8 wavelet basis. This wavelet would be used to compute one point in the resolution level 3 detail vector of a DWT.

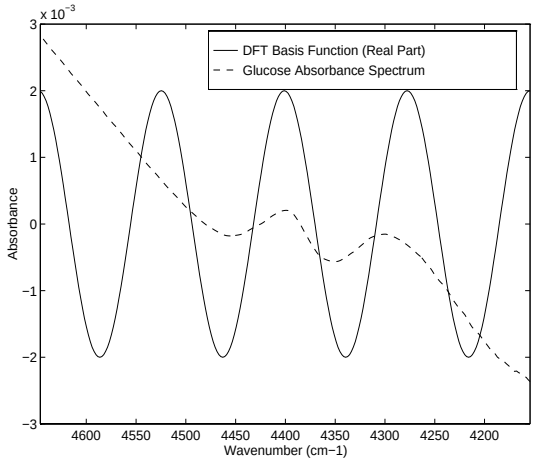

Figure 6. 400mg/dL glucose absorbance spectrum and the real part of a scaled DFT basis function.

3. DWT ALGORITHM FOR FINDING LINEAR PREDICTION EQUATIONS

In order to obtain an equation for predicting glucose concentration, we use a data compression prediction method. In this type of method, a transform is used in order to concentrate the salient spectral information of a calibration set of spectra into a few transform variables. A linear regression equation is then found between these important transform variables and the known glucose concentrations of the solutions from which the calibration spectra were taken. Finally, the coefficients in this regression equation are used to calculate the coefficients of a linear equation that can be used to predict the glucose concentration of new absorbance spectra.

Specifically, the process of finding the linear prediction equation begins by collecting a calibration set of spectra from samples with known glucose concentration. All of these spectra are then put into the rows of a matrix $\mathbf{X}$. The glucose concentration of the samples from which each of these spectra were taken are put into a column vector $\mathbf{y}$. The matrix $\mathbf{X}$ and the column vector $\mathbf{y}$ are then centered in the following manner:

$$\bar{\mathbf{X}} = \mathbf{X} - \begin{bmatrix} 1 \\ | \\ 1 \end{bmatrix} \bar{\mathbf{x}}'$$

$$\bar{\mathbf{y}} = \mathbf{y} - \bar{y}$$

Next, the basis that will be used in the DWT must be chosen. As mentioned earlier, one way of choosing an appropriate basis is to simply look for a basis that contains some wavelets which match up well with the spectral signature of glucose in solution. Another more quantitative manner of choosing an appropriate basis would be to perform leave-one-out cross validation on the calibration spectra using several different wavelet bases. For each wavelet basis to be tested, this entire prediction algorithm would be applied several times using leave-one-out cross validation in order to find prediction errors. The basis that yielded the lowest average prediction error could then be used to calculate a prediction equation for use with new spectra.

Once an appropriate wavelet basis has been chosen, the basis functions of the basis are placed in the columns of the matrix $\mathbf{V}$. When $\bar{\mathbf{X}}$ and $\mathbf{V}$ are multiplied, a new matrix $\mathbf{T}$ is created.

$$\mathbf{T} = \bar{\mathbf{X}}\mathbf{V}$$

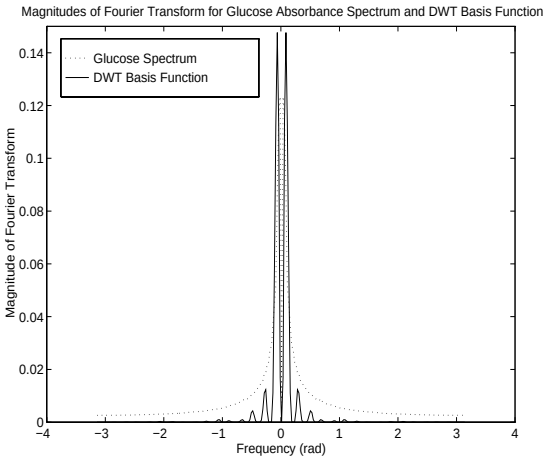

Figure 7. Magnitudes of the Fourier transforms of a 400mg/dL glucose absorbance spectra and of a D8 wavelet basis function that would be used to compute one point in the resolution level 2 detail vector of a DWT.

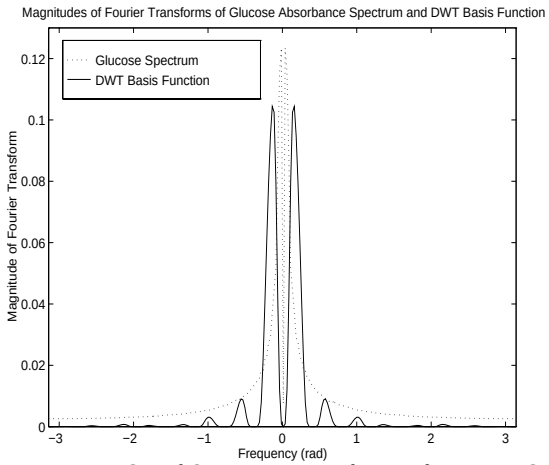

Figure 8. Magnitudes of the Fourier transforms of a 400mg/dL glucose absorbance spectra and of a D8 wavelet basis function that would be used to compute one point in the resolution level 3 detail vector of a DWT.

The rows of $\mathbf{T}$ contain the full DWTs of the spectra in $\bar{\mathbf{X}}$.

If the wavelet basis was well chosen, the important information in $\bar{\mathbf{X}}$ should be compressed into a few transform variables in $\mathbf{T}$. Thus, most of the information in $\mathbf{T}$ should be useless for prediction purposes. Indeed, this additional information can actually be deleterious to prediction results, since it only represents unwanted information that must be later filtered out. Thus, several transform variables in the DWTs found in $\mathbf{T}$ are eliminated from further use. The elimination of these variables compresses the transformed signals, which is why this method is called a data compression prediction method.

Choosing which variables to keep in this prediction process could be done in many different ways. We decided which transform variables to keep based on the frequency content of their resolution level. If a resolution level contained frequency information that matched up well with the frequency content of the spectrum of glucose in solution, then all of the transform variables in that resolution level were included in the future steps of this process. The magnitude frequency content of a 400mg/dL glucose spectrum and that of the D8 DWT basis functions of the resolution level 2 detail vector are shown in Figure 7. The magnitude frequency content of the glucose spectrum and that of the basis functions of the resolution level 3 detail vector are shown in Figure 8. Both Figures 7 and 8 show large regions of overlap between the frequency content of the glucose signal and that of the basis functions. Thus, in our studies the detail vectors of resolution levels 2 and 3 were regularly chosen to be used in the later steps of this prediction method. Instead of using this qualitative method of choosing which parts of the DWT should be kept for later steps, a more quantitative cross validation procedure could also be used.

Once certain transform variables have been chosen to be used in the rest of this process, these transform variables are stored in the matrix $\mathbf{T_c}$. This matrix can be found in the following manner,

$$\mathbf{T_c} = \bar{\mathbf{X}}\mathbf{V_c}$$

where $\mathbf{V_c}$ has as its columns those basis functions which are used to calculate only the chosen transform variables.

So long as the number of points in the spectra in $\mathbf{T_c}$ is less than the number of spectra in $\mathbf{T}$, a least squares regression equation can be found between the variables in $\mathbf{T_c}$ and the centered glucose concentrations in $\mathbf{y}$. The coefficients of this regression equation are the elements of the vector $\mathbf{q}$, which is calculated in the following manner:

$$\mathbf{q} = (\mathbf{T}_c'\mathbf{T}_c)^{-1}\mathbf{T}_c'\bar{\mathbf{y}}$$

Once we have found this vector q, we have all of the information necessary in order to build a linear prediction equation of the following form:

$$y_{pred} = b_0 + b_1 x_1 + b_2 x_2 + \ldots + b_{N-1} x_{N-1} = b_0 + \mathbf{x}'\mathbf{b}$$

In this equation y_{pred} represents the predicted glucose concentration. The x variables represent the data points in an absorbance spectra not in $\mathbf{X}$, and the b variables are regression coefficients. The vector $\mathbf{b}$ and the scalar b_0 can be found in the following manner,

$$\mathbf{b} = \mathbf{V_c q} = \mathbf{V_c}(\mathbf{T}_c'\mathbf{T}_c)^{-1}\mathbf{T_c}'\bar{\mathbf{y}}$$

$$b_0 = \bar{y} - \bar{\mathbf{x}}'\mathbf{b}$$

where $\bar{\mathbf{x}}$' is the mean spectrum of the spectra in $\mathbf{X}$ which was found when $\mathbf{X}$ was centered, and $\bar{y}$ is the mean value of $\mathbf{y}$ found when $\mathbf{y}$ was centered.

4. APPARATUS

All spectra were collected using a BOMEM Michelson MB-155 spectrometer with GRAMS/386 software for windows. The spectrometer was configured with an InAs detector, a KCl beamsplitter, and an external NIR source. The spectrometer was set to yield spectra covering the wavenumber range of 10,000cm^{-1} to 4000cm^{-1} with a resolution of 4cm^{-1}. These spectra were originally acquired as single-beam 31,956 point double-sided interferograms based on 128 coadded scans. The interferograms were then cosine apodized and Fourier transformed to produce single-beam spectra with 1.9cm^{-1} point spacing in the wavenumber range from 10,000cm^{-1} to 4,000cm^{-1}.

For all measurements, an optical interference filter was placed in the light path about a centimeter before the sample chamber so that the A/D converter of the spectrometer could be used as effectively as possible. This interference filter nominally passes light from 5000cm-1 to 4000cm-1 with transmission in the pass region ranging from 85-90%.

The following method for controlling sample temperature was employed. First, a 3-foot-long Cole-Parmer electrical heating cord was wrapped around the outer walls of the metal containment chamber several times. Next, a K-type thermocouple was attached to the inner wall of the chamber as close to the sample cell as possible. The temperature of the containment chamber was then controlled using the heating cord and thermocouple in conjunction with an Omega CN7600 temperature controller. The containment chamber was held at a constant temperature (+/- 0.3^{o}C) for a period of time long enough for the chamber and the sample to reach an equilibrium temperature.

All processing of spectral data will took place using MATLAB 4.1 for UNIX. For wavelet analysis, WaveLab .701 was used in conjunction with MATLAB. It is publicly available at http://playfair.stanford.edu:80/~wavelab.

5. RESULTS AND DISCUSSION

84 NIR absorbance spectra were collected using an FTIR spectrometer. 36 of these spectra were collected from solutions containing 40g/L bovine serum albumin (BSA). These solutions were prepared with glucose concentrations ranging from 20-400mg/dL, and their spectra were acquired at temperatures ranging from 35-39^{o}C. Another 36 spectra were collected from solutions containing 50g/L BSA. These solutions were prepared with glucose concentrations ranging from 20-400mg/dL, and their spectra were acquired at temperatures ranging from 34-40^{o}C. The final 12 spectra were collected from solutions containing 60g/L BSA. These solutions also were prepared with glucose concentrations ranging from 20-400mg/dL, but their spectra were always acquired at 37^{o}C.

The 84 spectra were all truncated around 4400cm^{-1}, so that they contained 256 points and covered the wavenumber range from about 4550cm^{-1} to 4150cm^{-1}. This region of the NIR spectra was chosen for our studies since it is known to contain glucose peaks, and since it is a region of relatively low water absorption[3]. Several truncated absorbance spectra are shown in Fig-

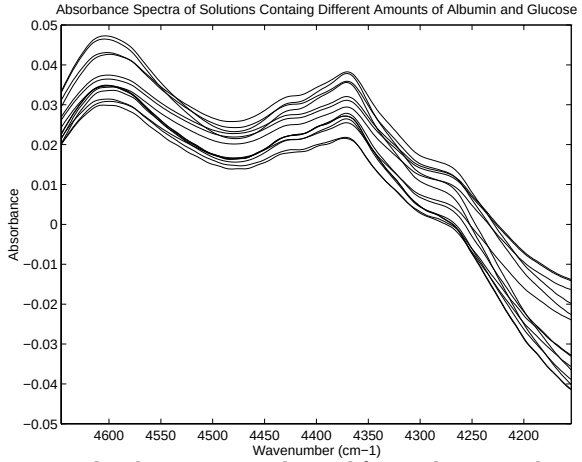

Figure 9. Absorbance spectra obtained from solutions with protein concentrations ranging from 40-60g/L, glucose concentrations ranging from 20-400mg/dL, and temperatures ranging from 34-40^{o}C.

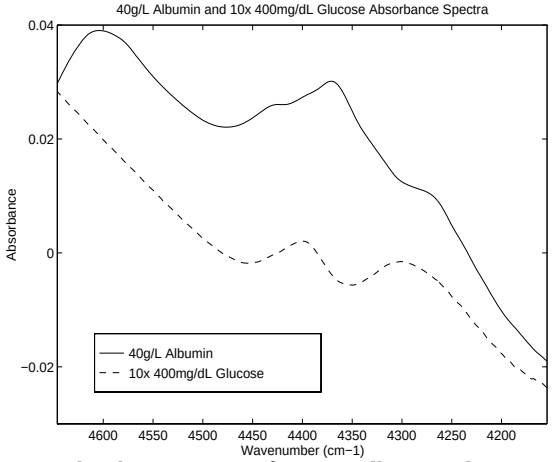

Figure 10. Absorbance spectra of a 40g/L albumin solution and of a 400mg/dL glucose solution. The glucose absorbance spectra was multiplied by 10 so that the two spectra could be shown on the same graph.

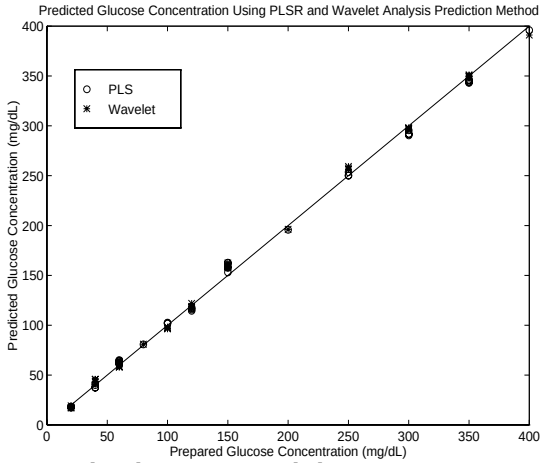

Figure 11. Predicted versus prepared glucose concentration using PLSR and the wavelet analysis prediction method described in this paper.

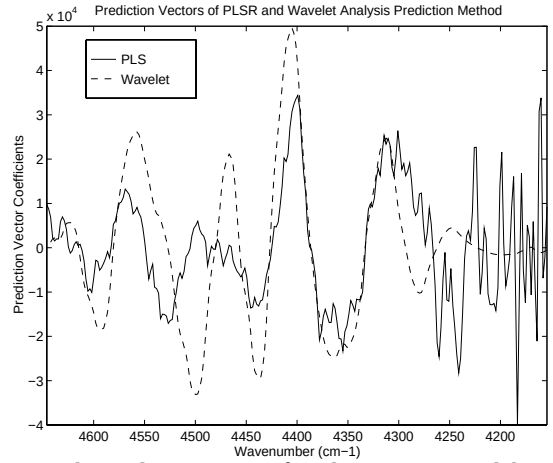

Figure 12. The prediction vectors found using PLSR and the wavelet analysis prediction method described in this paper. The vectors are plotted against the wavenumber range of the spectra in the calibration and prediction sets.

ure 9. Figure 10 shows the absorbance spectra of 400mg/dL glucose and 40g/Lalbumin. It should be apparent from inspection of Figures 9 and 10 that the spectra of Figure 9 are dominated by the spectral signature of albumin. In order to predict glucose concentration from the spectra in Figure 9, a spectral processing technique must be employed that can effectively separate the large albumin peaks from the much smaller glucose peaks.

In order to test the wavelet analysis prediction method, the 84 truncated absorbance spectra were divided into two data sets, a calibration set and a prediction set, each containing 42 spectra. Both data sets contained spectra obtained from solutions covering the full range of glucose concentrations, albumin concentrations, and temperatures. No spectra in the prediction set, however, had the same glucose concentration and protein concentration as any spectra in the calibration set.

The calibration data set was used to build a linear prediction equation using the wavelet analysis process described above. The wavelet basis used in the creation of the prediction equation was chosen to be the D8 basis, since this basis seemed to have some basis functions that matched up well with the spectral signature of glucose (see Figure 5). Resolution levels 2-3 of the DWT were used in order to form our prediction equation since these resolution levels contained frequency bands that were present in the spectral signature of glucose in solution (see Figures 7-8).

Once a linear prediction equation was found, this equation was applied to the spectra in the prediction set. The results of using this prediction method are shown in Figure 11. Figure 11 also displays the results of using partial least-squares regres-

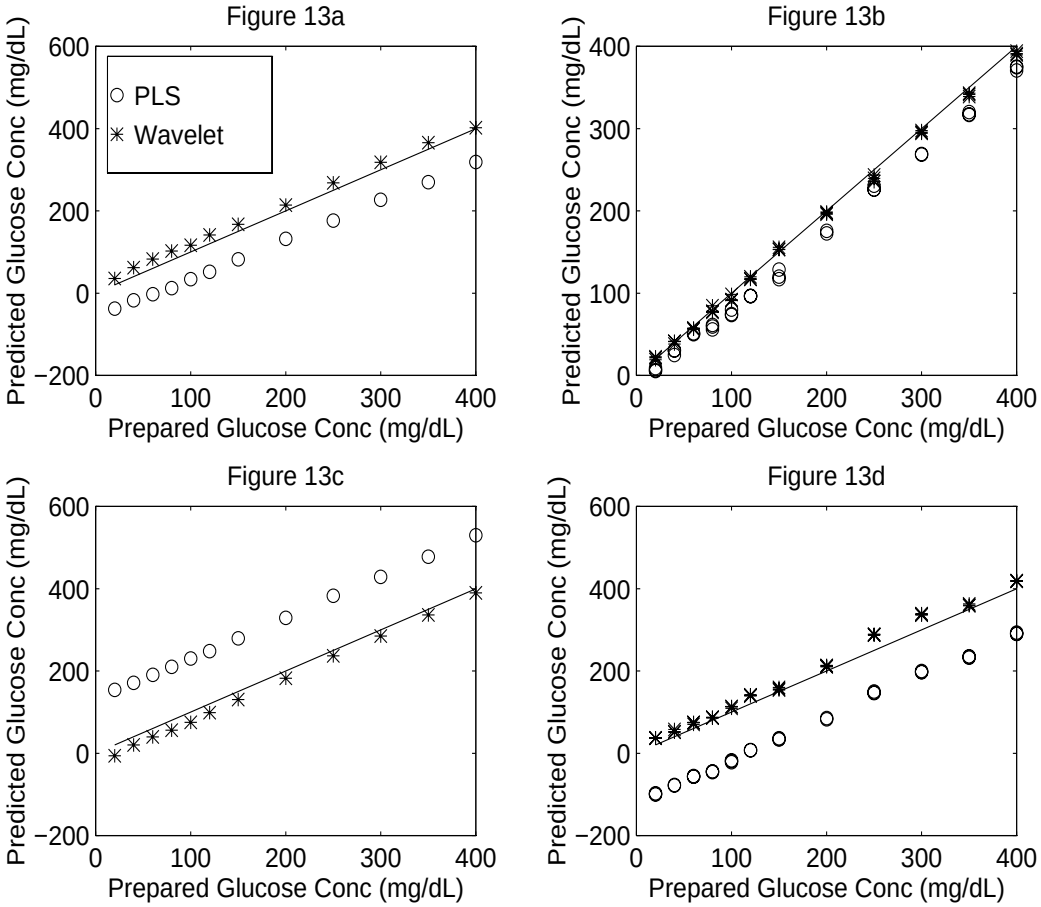

Figure 13. Predicted versus prepared glucose concentration using PLSR and the wavelet analysis prediction method described in this paper. Different calibration and prediction set combinations were used to create each plot. Each calibration set and predictions set contained spectra obtained from solutions with the same albumin concentration. Figure 13a: 40g/L albumin calibration set, 60g/L albumin prediction set. Figure 13b: 40g/L albumin calibration set, 50 g/L albumin prediction set. Figure 13c: 50g/L albumin calibration set, 60g/L albumin prediction set. Figure 13d: 50g/L albumin calibration set, 40g/L albumin prediction set.

sion (PLSR) on the same calibration and prediction data sets. PLSR is described in detail in multivariate processing and calibration literature[8]. Both PLSR and the wavelet analysis prediction method predicted glucose concentration quite well, even with varying protein concentrations. The RMSEP using PLSR was 5.38. The RMSEP using the wavelet analysis technique was 4.96.

Figure 12 shows the prediction vectors (**b** vectors in the linear prediction equations) that were found using both the wavelet analysis and the PLSR prediction techniques. Both prediction vectors have significant peaks around 4400cm-1, which is where the primary glucose absorbance peak occurs. These prediction vectors are characteristic of the vectors that were usually yielded when PLSR and the wavelet analysis technique were used to predict glucose concentration. The prediction vectors of PLSR often had significant amounts of high-frequency variation, which had no obvious correlation to the spectrum of glucose in solution. The prediction vectors of the wavelet analysis method, on the other hand, often had large lobes which were seemingly uncorrelated with the glucose spectral signature.

In this first example, the wavelet analysis technique worked fairly well, yielding comparable results to those found from PLSR. This example does not, however, fully represent the predictive ability of the wavelet analysis method. The D8 basis was chosen for use in this example because it seemed to be an appropriate basis for glucose concentration prediction, and since the Daubechies bases are popular in application. Other wavelet bases, however, can be chosen, as well as other combinations of resolution level detail and approximation vectors. For example, when the wavelet analysis prediction process was implemented using the D10 wavelet basis, this yielded an RMSEP was 4.77. As another example, when the detail vectors of resolution level 2-4 were used with the D8 basis, the RMSEP was 4.89. With a larger data set, it would be possible to implement this

prediction algorithm using thousands of different combinations of bases and resolution levels and probably find some combinations that consistently outperform others.

One specific example where the wavelet analysis prediction algorithm was found to significantly outperform PLSR was when the calibration set used to create prediction equations contained spectra collected from solutions with the same protein concentration. When the prediction equations were then used on spectra collected from solutions with protein concentrations different from that of the calibration set, the wavelet analysis prediction algorithm could significantly outperform PLSR with the right choice of basis and transform variables. The plots in Figure 13 display the results yielded by the wavelet prediction technique and PLSR for four different choices of calibration and prediction sets. In all of these cases, the wavelet prediction algorithm was implemented using the detail vectors of resolution levels 2-4 of the D8 basis. In Figures 13a and 13b, the 36 40g/L-albumin spectra were used as the calibration set to build a prediction equation. Figure 13a shows the results when the 12 60g/L-albumin spectra were used as the prediction set. Figure 13b shows the results when the 36 50g/L-albumin spectra were used as the prediction set. In Figures 13c and 13d the 50g/L-albumin spectra were used as the calibration set to build a prediction equation. Figure 13c shows the results when the 60g/L-albumin spectra were used as the prediction spectra, and Figure 13d shows the results when the 50g/L-albumin spectra were used as the prediction spectra. These plots clearly display that the wavelet prediction algorithm performs better than PLSR when unmodelled albumin concentration fluctuation is present in the prediction set.

Currently, we have no clear explanation as to why the wavelet prediction algorithm performs so much better than PLS in this case. It is important for us to note that the wavelet prediction algorithm does not perform nearly as well when bases other than D8 are used. This intriguing observation definitely warrants more investigation into answering the question of why the D8 DWT performs so well. Indeed, the initial results of using the wavelet analysis prediction method were successful enough to warrant the additional research of several aspects of using the DWT in glucose concentration prediction algorithms. Most importantly, additional research is necessary in the area of finding better ways to choose which wavelet basis and transform variables to use when implementing the wavelet analysis prediction method.

6. REFERENCES

1. S. Pan, H. Chung, M. A. Arnold, G. W. Small, “Near-Infrared Spectroscopic Measurement of Physiological Glucose Levels in Variable Matrices of Protein and Triglycerides”, *Analytical Chemistry* **68**, pp.1124-1135, 1996.

2. H. Chung, M. A. Arnold, M. Rhiel, and D. W. Murhammer, “Simultaneous Measurements of Glucose, Glutamine, Ammonia, Lactate, and Glutamate in Aqueous Solutions by Near-Infrared Spectroscopy”, *Applied Spectroscopy* **50**, pp. 270-276, 1996.

3. M. A. Arnold and G. W. Small, “Determination of Physiological Levels of Glucose in an Aqueuos Matrix with Digitally Filtered Fourier Transform Near-Infrared Spectra”, *Analytical Chemistry* **62**, pp.1457-1464, 1990.

4. L. A. Marquarst, M. A. Arnold, and G.W. Small, “Near-Infrared Spectroscopic Measurement of Glucose in a Protein Matrix”, *Analytical Chemistry* **65,** pp.3271-3276, 1993.

5. C. Fischbacher, K. U. Jagemann, K. Danzer, U. A. Muller, L. Papenkordt, J. Schuler, “Enhancing calibration models for non-invasive near-infrared spectroscopial blood glucose determination”, *Fresenius J Analytical Chemistry* **359**, pp. 78-82, 1997.

6. A. Graps, “An Introduction to Wavelets”, *IEEE Computational Science and Engineering* **2**, 1995.

7. G. Strang and T. Nguyen, *Wavelets and Filter Banks*, Wellesley-Cambridge Press, Wellesley MA, 1996.

8. H. Martens and T. Naes, *Multivariate Calibration*, John Wiley & Sons, New York NY, 1989.